

Impacts of Climate Change on the Nile Flows at Dongola Using Statistical Downscaled GCM Scenarios

Mohamed E. Elshamy¹, Mohamed A.-A. Sayed², Bakr Badawy³

¹ Nile Forecast Center, Ministry of Water Resources and Irrigation, Egypt

² Regional Coordinator, Eastern Nile Planning Model, ENTRO, Ethiopia

³ PhD Student, Max-Planck Institute for Biogeochemistry, Jena, Germany

Abstract

This study was initiated with the objective of evaluating the relative magnitude of uncertainties across emission scenarios, due to downscaling. The study analyzed the change in Nile flows at Dongola resulting from two emission scenarios (A2 and B2) using the results of 3 GCMs (CGCM2, ECHAM4, and HadCM3). It is to be mentioned here that a GCM is a global circulation model (GCM) that could depict different pictures for the future precipitation over the Nile basin, and consequently could expect the discharge of the river.

A 10-member assemblies of statistically downscaled precipitation scenarios for the 2010–2099 period was designed for the whole Nile basin from the output of these experiments. Potential evapotranspiration (PET) were calculated for the base-period (1961-1990) and for three 30-year time slices in the future (2010-2039, 2040-2069, and 2070-2099) using the Penman-Montheith equation. Rainfall and PET scenarios were used to drive a fine-scale hydrological model of the Nile Basin. Observed rainfall from the base-period was used to determine the parameters of the statistical downscaling model (SDM) for the different GCMs.

The results showed that the ECHAM4 predicts a steady increase in Nile flows in the future while CGCM2 underestimates the flow in the base-period. On the other hand, an increase was predicted by years 2020 and 2030. The expected flow is similar to the observed mean. It was also predicted that the flow might decrease rapidly in case of the A2 scenario. However, the HadCM3 showed a slight trend of increase to the flood season flows and a slight trend of increase for the base-period flow. This counterbalances each other so that the total annual flow does not change. The results also indicated that the uncertainty range, across the models, is larger than that across the two studied scenarios. The range of differences between the scenarios is model dependent and time dependent. The uncertainty due to downscaling is also large and is proportional to the flow. It was thus concluded that the implications of the changes might be huge for the water resources planning and management within the basin and particularly for Egypt.

Key words: Nile Basin, Hydrologic Models, Climate Scenarios, Downscaling, Climate Change Impacts

1. INTRODUCTION

Climate fluctuations dramatically change the structure and the regime of the Nile River. It is only within the near future, that the Nile might change its current hydrologic characteristics and its connectivity between Equatorial Africa and the Mediterranean Sea (Said, 1993). The unique hydro-climatic characteristics of both the equatorial Lakes and the Ethiopian Plateaux make them sensitive to climate variability. The Equatorial Lakes region has exhibited particular sensitivity to marginal changes in precipitation in the early 1960s. This caused the level of Victoria to rise by 2.5m (Kite, 1981). The runoff across many regions of the Nile Basin is very sensitive to climate variations related to global circulation patterns. Increased atmospheric concentrations of greenhouse gases are expected to change these global circulation patterns. Anthropogenic climatic change might cause significant variation in the Nile flows. Figure 1) shows a general map of the Nile River.

2. LITERATURE REVIEW

From the literature, clear was that a number of researchers investigated the implications of fluctuations in Nile discharge for water resources in Egypt, particularly since the prolonged period of low flows during the 1970s and 1980s (e.g. Abu-Zeid and Biswas, 1991; Conway and Hulme, 1993). The

historical fluctuations in the Nile River discharge was reviewed by Shahin (1985), Evans (1990), Sutcliffe and Lazenby (1990) and Sutcliffe and Parks (1999). Some of these fluctuations were linked to the ENSO phenomenon (e.g. Eltahir, 1996) especially those originating from the Blue Nile. Conway and Hulme (1993) showed that Blue Nile and White Nile flows are not correlated but confirmed the correlation between Blue Nile flows and Sahelian precipitation which is influenced by the ENSO phenomenon.

Also from the literature, clear was that several attempts evaluated the sensitivity of the Nile discharge to the temperature changes (or evaporation) and precipitation. Probably the first of these studies was by Kite and Waititu (1981) who looked at the Nzoia River, a tributary of Lake Victoria, using the Sacramento Watershed catchment model. They found that the streamflow is highly sensitive to precipitation (i.e. a 10% increase in precipitation caused a 40% increase in the runoff, in other words, the relationship is non-linear). Compared to precipitation, runoff is less sensitive to changes in potential evapotranspiration (PET) but still, a change of 6% in the PET causes more than 10% change in the runoff. Similar results were reported by several authors for Victoria Lake (e.g. Conway and Hulme, 1996; Sene et al., 2001) and for the Blue Nile (e.g. Conway and Hulme, 1996; Sayed, 2004).



Figure 1: Nile basin map (from www.nilebasin.org)

Meanwhile, Global Circulation Models (GCMs) show different pictures of climate change over the Nile Basin, while they agree on the temperature rise. On the other hand, they disagree on the direction of precipitation change. Analysis of 16 transient experiments (using different emission scenarios) from 7 different GCMs by Elshamy (2000) revealed an average increase in temperature over the basin by 2-4.3°C by year 2050. Temperature changes were not uniform over the basin, with higher temperature rises in more arid regions of Northern Sudan and most of Egypt and lower rises around the equator. Although most of the analyzed experiments showed an increase in precipitation over the basin (of up to 18%), some experiments showed a reduction (of up to 22%), while one experiment showed almost no change. Hulme et al. (2001) conducted an extensive study of climate change over Africa between 1900 and 2100 using observed and GCM results for SRES (IPCC, 2000) emission scenarios. For Ethiopia, the expected change in annual rainfall varied between -10 and +25% by the year 2050 depending on the model and the emission scenario. The range of changes for the rainy season was in the order of 100%.

Even with an increase in the basin rainfall, river runoff might decrease. This is attributed to the fact that the expected increase in the evaporation demand is due to the temperature rise. Based on future climate change, scenarios from two versions of the Hadley Centre GCM, Arnell (1999) estimated that the increase in the evaporation demand might counterbalance the increase in the basin rainfall so that the runoff will remain virtually unchanged.

The high sensitivity of the basin to climatic drivers combined with the disagreement of GCMs regarding the direction of precipitation change has resulted in a very wide range of expectations for streamflow. Strzepek et al. (1995) showed a very wide range of flow changes (-77% to +30%) in response to climatic changes taken from 3 old generations of GCMs. Yates (1996) used 3 equilibrium experiments (of CO₂ doubling) and 1 transient experiment. He showed a wide range of changes for the Nile inflows. 3 of the models indicated increases in natural river flow at Aswan for more than 50%, the fourth model showed a 12% reduction. Temperature rise was expected to be induced by increasing the evaporation losses from Nasser Lake, the same is expected for the case of increasing the irrigation water demands. The study predicted changes in the water availability to Egypt in the range between -11% to +61%.

Recently, Sayed (2004) suggested a positive relation between the rainfall and temperature in the Blue Nile Basin based on a comparison of temperature and mean areal precipitation between 1977 and 2003. In the White Nile region, this relation was weaker. Based on the results of the MAGICC/SCENGEN scenario generator (Raper and Cubasch, 1996), it was expected that the change in the rainfall, in the Blue Nile, would be 2 to 11% for year 2030. On the other hand, rainfall in the White Nile would increase 1 to 10% for the same year. The associated range of changes in the inflow to Nasser Lake is -14% to 32%.

In summary, there are large uncertainties in predicting climatic changes over the Nile basin and their impacts on its flows. In addition to the GCM uncertainties, their large spatial scales require downscaling of their climatic outputs in order to be used as inputs for hydrological models. There are two main categories of downscaling methods, dynamic and statistic.

3. DYNAMIC AND STATIC DOWNSCALING

Regarding the dynamic downscaling, as the name indicates, it aims at solving the downscaling problem using physical dynamics of the climate system. It uses the same atmospheric physics underlying GCMs to resolve the required meteorological variables in a limited region with the required spatial scale. This involves one-way nesting of higher-resolution Regional Climate Models (RCMs) within GCMs to improve the simulated regional features of climate. In this case, the GCM provides initial and time-varying boundary conditions to the RCM. This provides detailed climatic simulation of the area of interest. Mohamed et al. (2005) was the first to apply a regional climate model to the Nile Basin. He applied a modified version of the RACMO, the limited area model used by KNMI (The Royal Netherlands Meteorological Institute) to study the impacts of the Sudd wetland on the Nile hydroclimatology. Soliman et al. (2008) applied RegCM3 (another regional climate model) to a window within the Nile basin covering the Sobat and the Blue Nile sub-basins. The study used different rainfall and temperature datasets to validate the outputs of the RCM over the region.

As for the statistic or empirical downscaling, it relies on the observed historical climate to develop relationships between the required downscaled variables (usually surface variables such as temperature and precipitation) and the reliable large-scale meteorological features produced by GCMs such as sea level pressure and geopotential heights. This implies a debatable assumption about the stability of such relationships under altered climate. It also depends on how well these large scale features are simulated by GCMs. Empirical methods have the advantage of generating assemblies of downscaled variables, which allows the assessment of the additional uncertainty introduced by downscaling (Bárdossy, 2000). They require only modest computational resources and could be used to assess scenarios from different GCMs.

This study uses a statistical downscaling model to construct detailed precipitation scenarios for the whole Nile Basin. The rainfall scenarios have been downscaled to the fine resolution required by the Nile Forecast System (NFS - Nile Forecast Center, 2007) and temporally disaggregated from the monthly to the daily time step. Potential (reference crop) evapotranspiration (PET) scenarios were designed from the GCM output to be consistent with rainfall. Previous studies used simpler methods to

calculate future PET; e.g. Conway and Hulme (1996) assumed a 4% increase in PET per degree increase in temperature.

In this study, using the physically-based FAO Penman-Monteith method (Allen et al., 1998), the assumption of pure temperature dependence of PET was evaluated. The NFS was then used to translate these rainfall and PET scenarios to flow scenarios at Dongola to project the impacts of the developed scenarios on the Nile inflow to Nasser Lake. The study downscaled the results of 3 GCMs for 2 SRES emission scenarios (A2 and B2) and, through assemblies, attempts showed the relative uncertainty due to emission scenarios, GCMs, and downscaling. For each GCM/scenario combination, an assembly (set) of ten members was generated through random sampling of the temporal disaggregation scheme which is part of the downscaling model.

4. METHODS AND DATASETS

The IPCC data distribution centre provides results of several GCMs for a number of the SRES scenarios for many atmospheric variables. Monthly time series data for the A2 and B2 scenarios for the baseline period 1961-1990 and the future period 2010-2100 were downloaded from the IPCC Data Distribution Centre for 3 Atmosphere-Ocean Coupled General Circulation Models, namely:

- second-generation ocean-atmosphere model CGCM2 developed by the Canadian Climate Modelling Centre
- fourth generation ocean-atmosphere model ECHAM4 developed at the Max Planck Institute, Germany
- third generation ocean-atmosphere model HadCM3 developed at the Hedley Center, UK

4.1 Rainfall

Observed rainfall was obtained from the NFS database, which is an integral part of the NFS software (Nile Forecast Center, 2007) and consisted of daily gridded fields of merged satellite and gauge rainfall estimates at 20 km resolution for the period 1992-2001 (refer to (Elshamy, 2006) for further details). The selected GCMs were able to reproduce the annual observed rainfall volumes with reasonable accuracy. In addition, the GCM rainfall distribution during the year was well reproduced. According to the three GCMs, rainfall is distributed mainly south of the basin (Equatorial Lakes) during the months of November till February. Then there is a northward migration during April and May and this peaks during June till September over the Ethiopian highlands. Thus, the rainfall is oscillating about the Equator. This suggests that these GCMs correctly predict the rainfall dependence upon the position of the Inter-Tropical Convergence Zone (ITCZ).

The Statistic Downscaling Model (SDM) developed during Nasser Lake Flood and Drought Control project (LNFDC, 2008) was used to downscale the coarse-resolution monthly precipitation time series into fine-resolution (at the NFS resolution, i.e. daily series). This model uses the large-scale GCM precipitation fields as a predictor for the local-scale rainfall. As precipitation is not explicitly simulated by GCMs, and is based on other internally calculated variables such as sea-level pressure, errors in rainfall simulations result from errors in the driving variables which are more commonly used as predictors than precipitation. Widmann et al. (2003) showed that the GCM-simulated rainfall could be a good predictor to the small-scale rainfall. Furthermore, they noted that the rainfall predictor outperformed other commonly adopted predictors such as 1000-hPa geopotential height. Salathé (2005) successfully used the 'local scaling' method developed by Widmann et al. (2003) to downscale GCM rainfall to a 15 km resolution (daily time-step) for a mountainous river basin in Washington, USA.

The statistical downscaling model is formulated by establishing relationships between GCM monthly precipitation values and the statistical properties (probability of a wet day following a dry day P_{wd} , probability of a wet day following a wet day P_{ww} , and the mean daily rainfall rate M_{rr}) of 31 rain gauges distributed over the Nile basin for the period 1992-2001. This is the period with the most complete dataset at the time of the analysis. The distributed hydrological model (described below) requires gridded precipitation data as input (20 km resolution). These rainfall data were generated using a multidimensional stochastic rainfall generator based on the Turning Bands method (Mantoglou and Wilson, 1982). The generator produces synthetic sequences of daily rainfall reproducing the spatial and temporal structure of historical rainfall. The former was represented using a homogeneous and isotropic exponential models for spatial covariance while the latter was modeled using the parameters; P_{ww} ,

Pwd derived above. The rainfall distribution on a rainy day was modeled using a two-parameter gamma distribution scaled by Mrr. The orographic rainfall component associated with the Ethiopian Highlands was modeled using a spatially-varying multiplicative factor derived by comparing the long-term averages of observed and uncorrected simulated rainfall over the baseline period for each 20 km grid square. 10 assembled members were generated for each of the 6 GCM/emission scenario combinations by varying the initial seed of the random number generator used in the stochastic rainfall generator.

4.2 Evapotranspiration

Mean monthly PET was calculated for the 1961-1990 base-period and for the three 30-year future time slices (2010-2039, 2040-2069, 2070-2099) using FAO Penman-Monteith method (Allen et al., 1998) for each GCM and scenario. 30-year mean monthly GCM outputs of temperature, vapour pressure (or dew point temperature), wind speed, and radiation over the respective time slices were downloaded from the IPCC data distribution centre and used in the calculations. To remove the bias of the GCM, the future (scenario) PETScen grids were calculated as:

$$\text{PETScen} = \text{PETNFS} * \text{PETGCM-Scen} / \text{PETGCM-Base}$$

where

PETscen: Future PET scenario

PETNFS: NFS long-term monthly PET

PETGCM-Scen: Calculated PET for the selected GCM, emissions' scenario, and time slice

PETGCM-Base: Calculated PET for the selected GCM for the base period 1961-1990

The mismatch between the rainfall base period (1992-2001) and the PET base period (1961-1990) was dictated by data availability. Hopefully, it might not be as important as one could think due to the little sensitivity of the NFS flows to PET variations as shown by Elshamy et al. (2008).

4.3 Streamflow

The NFS is then used to translate rainfall and PET scenarios into streamflow scenarios. The NFS is a real-time distributed hydro-meteorological forecast system designed for forecasting Nile flows at designated key points within the Nile. Of major interest is the inflow of the Nile into the Aswan High Dam, Egypt, as measured at Dongola. The system is hosted at the Nile Forecasting Center (NFC) of the Ministry of Water Resources and Irrigation (MWRI), Giza, Egypt. The core of the NFS is a conceptual distributed hydrological model of the whole Nile system including soil moisture accounting, hillslope and river routing, lakes, wetlands, and man-made reservoirs within the basin. Elshamy (2008) presented an evaluation of the long-term performance of the NFS and found that it could explain 76% of the observed monthly variance of Dongola flows over the period 1940-1999. Errors were related to the quality of rainfall and performance was generally better for the latter period of record after the establishment of the NFC and the utilization of satellite images to estimate rainfall. For more details about the NFS refer to Elshamy (2006) and LNFDC (2008).

In order to assess the impacts of the developed climate change scenarios, the simulated stream-flow at Dongola for each GCM/scenario combination is compared to GCM simulation for the base-period (1992-2001) to avoid the GCM bias in simulating current conditions. First the simulations of the base-period were assessed versus the observed stream-flow for the baseline period which mounted to 82.5 BCM.

5. ANALYSIS AND RESULTS

Results were obtained, analyzed and are represented here. These results are displayed for flows at Dongola for the baseline and future periods focusing on the mean annual hydrograph. The future changes by each GCM scenario are analyzed for total flow, flood season flow (during the months July – October), and baseflow (during the rest of the year). Changes in flood season flows are indicative of changes in the contribution of the Ethiopian Plateau tributaries (mainly Blue Nile and Atbara) while changes in the baseflow are indicative of changes in the contribution of the White Nile. The range of flows (maximum and minimum) across the 10 assemblies are used to indicate the uncertainty introduced by the SDM. The maximum and minimum are used rather than the mean \pm one or two standard deviations because of the relatively small sample size (only 10 assemblies). The SDM requires

a long time on a dedicated Linux PC to generate one assembly for the whole simulation period, therefore the number of assemblies was constrained by computing time. Uncertainties due to emission scenarios and climate models were also indicated by comparing the results of the A2 and B2 scenarios for each GCM, and across the 3 GCMs.

5.1 Base Period (1992-2001) Results

Figure 2 shows the mean monthly hydrographs for the 3 selected GCMs compared to the observed. Both HadCM3 and ECHAM4 slightly overestimate the rising limb and the peak of the hydrograph while CGCM2 underestimates the peak. Simulations of the base-flow component are closer for all models but CGCM2 still underestimates this. This indicates that most of the errors in ECHAM4 and HadCM3 occur for the Blue Nile and Atbara basins while CGCM2 has errors for those two sub-basins in addition to errors in the White Nile basin. However, this does not eliminate the possibility for compensating errors for ECHAM4 and HadCM3. The uncertainty bands generally encompass the observed hydrograph for the three models with narrower bands for CGCM2 than for the other two models. It seems that the width of the uncertainty band is proportional to the flow, which is understandable. Thus, it is smaller for CGCM2 compared to the other two models because it produces less flow, and is smaller for the base-flow than for flows during the flood season (July to October).

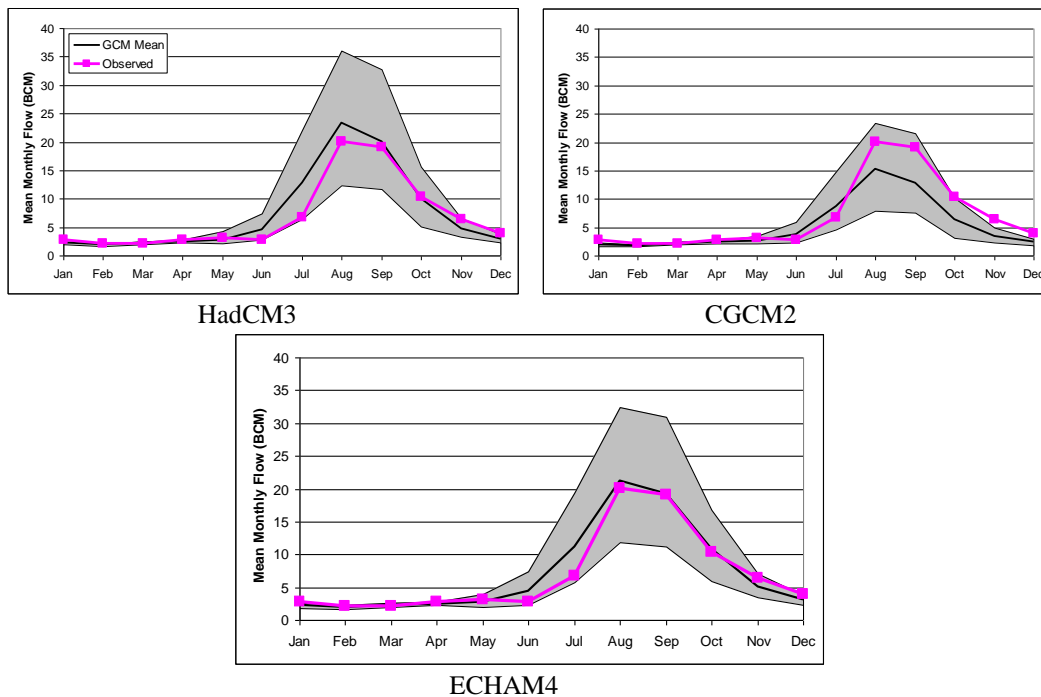
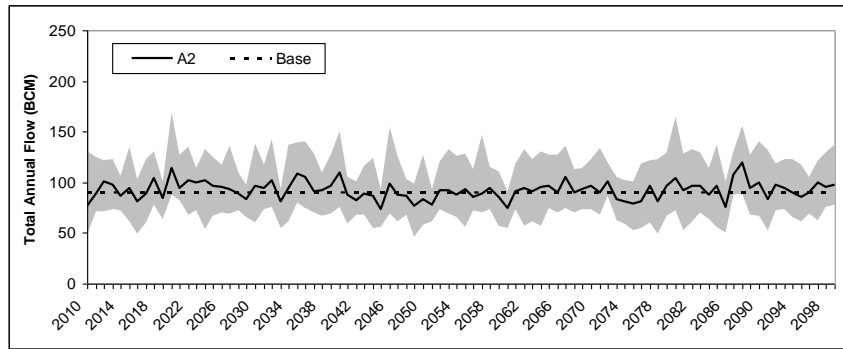


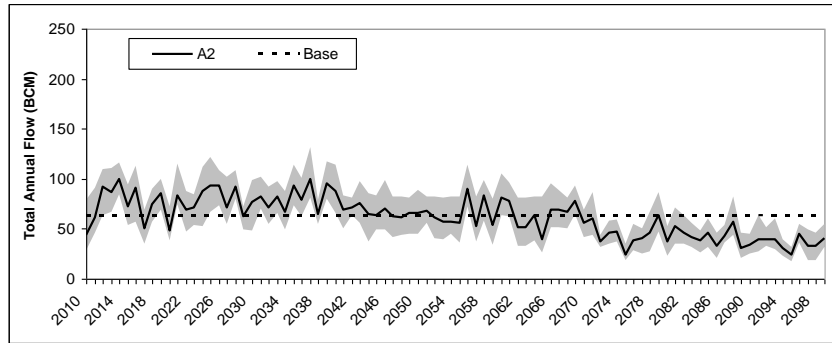
Figure 2: Simulated mean hydrographs at Dongola from 3 GCM experiments for the base period (1992-2001) Grey bands indicate the uncertainty range (maximum and minimum flows) across the 10 ensemble members

5.2. Future Trends Results

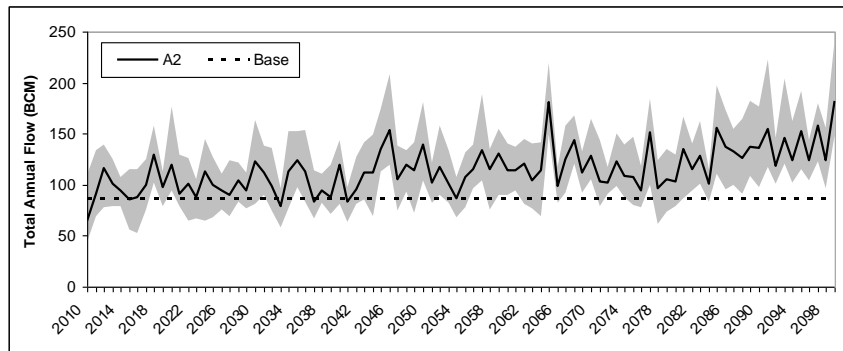
The comparisons were conducted with the mean across the 10 assemblies of each model for the base period (10 years) to minimize the effects of GCM errors on the predicted trends. For the scenario A2 (Figure 3), HadCM3 shows nearly no trends over the next century (2010-2099) as the mean annual flow series (of the 10 assemblies) fluctuates around the mean for the base period (10 years x 10 assemblies). For CGCM2, the annual flow at Dongola initially increases till around year 2040 then it is more or less stable until the middle of the 2060 ies. It starts a downward trend till the end of the century to reach only 61% of the mean for the base period. ECHAM4 showed a rising trend for most of the simulation period. Figure 4 shows the results for B2 emission scenarios which revealed similar but with less pronounced trends, i.e. generally downward trend for CGCM2, generally upward trend for ECHAM4, and fluctuations around the base-period mean for HadCM3. The uncertainty range is generally wide and is proportional to the mean annual flow as reported above.



HadCM3

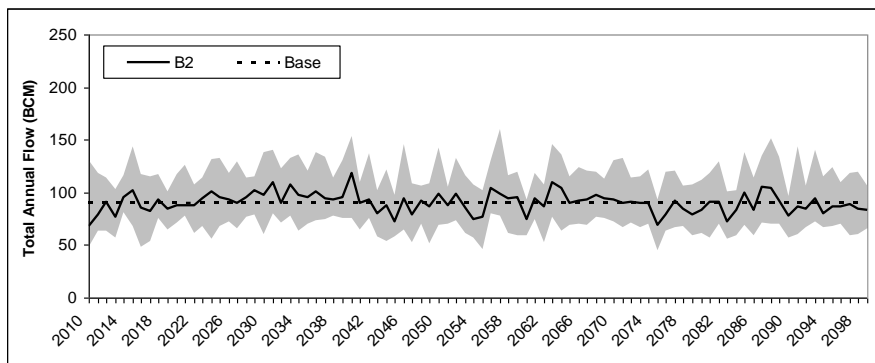


CGCM2



ECHAM4

Figure 3: Simulated annual flow series at Dongola from A2 experiments (2010-2099)



HadCM3

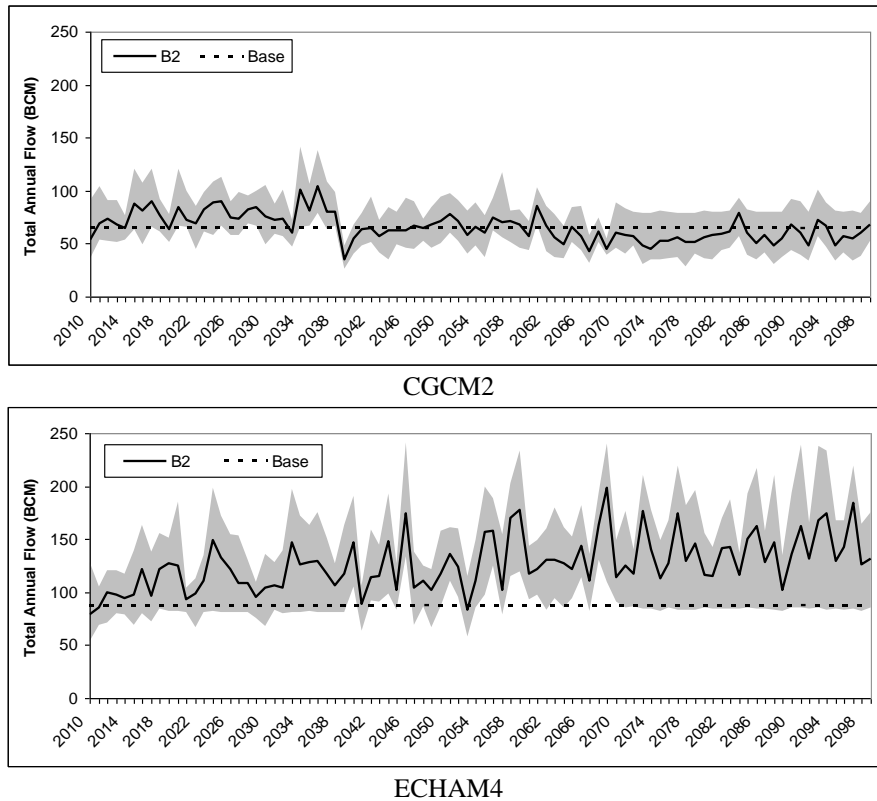
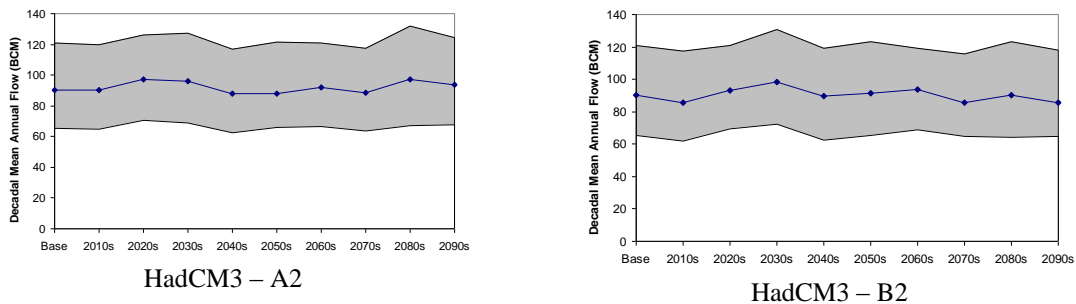


Figure 4: Simulated annual flow series at Dongola from B2 experiments (2010-2099)

To visualize the trends more clearly, the future period was divided into decades and the average values for each decade (for the mean, maximum, and minimum across the 10 assemblies) as well as the base period were represented and are given on figure (5). HadCM3 did not show significant changes from the base period for both A2 and B2 while ECHAM4 showed sustained increases in decadal means especially for B2. CGCM2 predicts decadal mean flows to initially increase under both A2 and B2 scenarios and then they are reduced but more rapidly under A2 compared to B2. The width of the SDM uncertainty band is large in all cases and increases with the decadal mean flow.

In order to investigate whether there are time-shifts in the hydrograph (e.g. changes in timing of the peak), decadal mean hydrographs were plotted and are given on Figure 6. Generally, the hydrographs are scaled up or down depending on the GCM and scenario combinations indicating no major changes in the timing of the peak at Dongola (August). However, CGCM2 predicts that the peak flow may delay till September in some decades under scenario A2. ECHAM4 predicts similar changes but to a smaller extent under scenario A2, as well. The observed mean hydrograph for the base period, Figure 2) showed a flatter peak extending till September and thus, these changes could be considered minor.



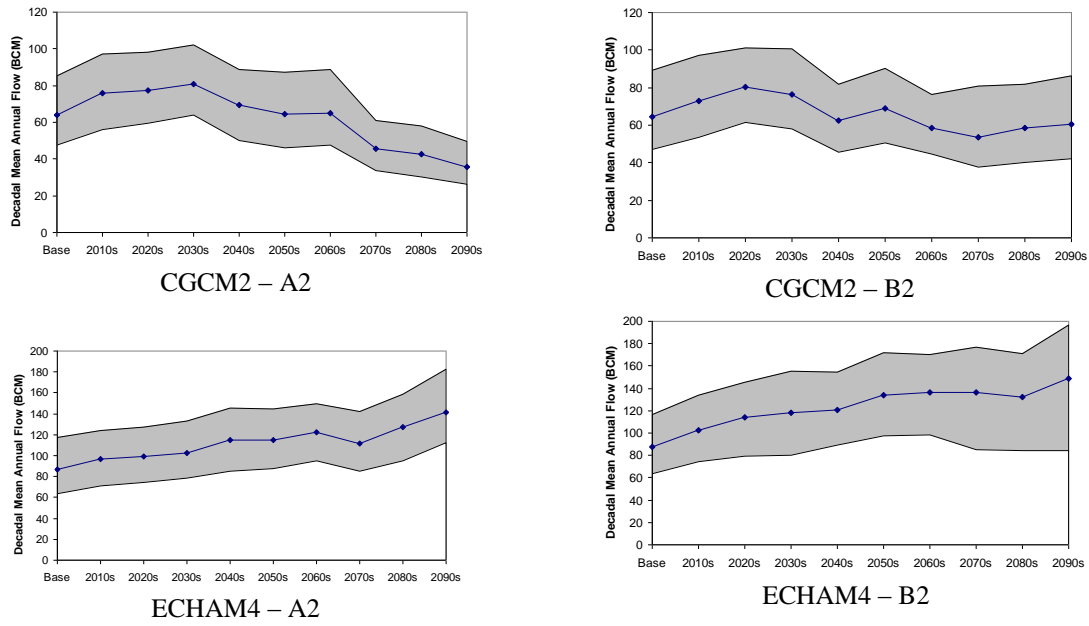


Figure5: Simulated decadal mean annual flow at Dongola from 6 GCM experiments
 Grey band indicates the uncertainty range (maximum and minimum flows) across the 10 assemblies

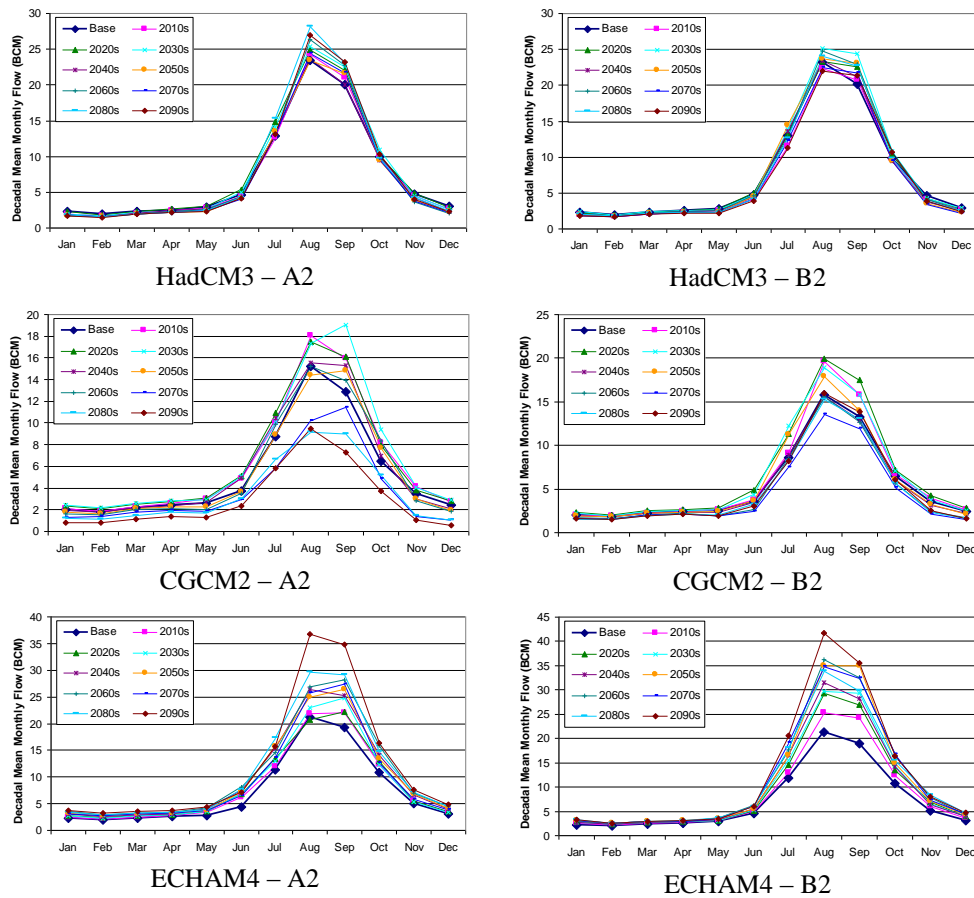


Figure 6: Simulated decadal mean hydrographs at Dongola from 6 GCM experiments

Figure 7 shows the future trends of changes for the flood season flows (July – October) which are indicative to the changes in the Blue Nile and Atbara flows. In general, the trends are similar to those seen above for the total annual flows. HadCM3 B2 flows fluctuate around the mean for the base period while there is a slight upward trend under A2. CGCM2 shows initial increases under A2 scenario followed by large reductions. Under B2, CGCM2 shows smaller initial increases compared to A2 but then decadal mean flows were reduced and then stabilize at nearly the base-period value. ECHAM4 showed upward trends for flows under both scenarios but the rate of increase was faster under A2.

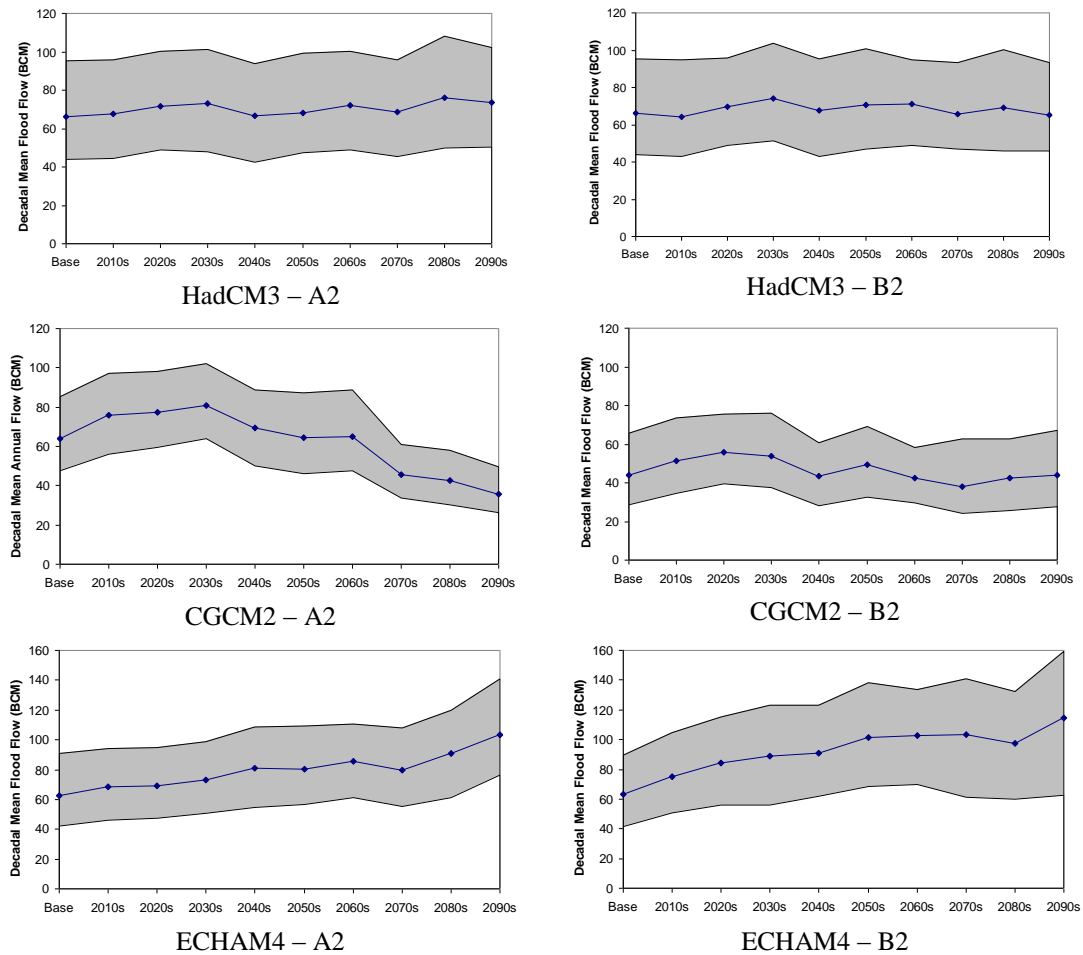


Figure 7: Simulated decadal mean flood flow at Dongola from 6 GCM experiments

The future trends for the base-flow component (November – June) are shown on Figure 8 as a surrogate of White Nile flows. In this case, HadCM3 showed a slight downward trend under both scenarios but because the base-flow component is generally smaller than the flood component, there is no discernable trend for HadCM3 for total flow. The contribution of the flood season flow to the total annual flow increases from 73% for the base-period to 79% and 76% for the 2090s under A2 and B2, respectively. CGCM2 showed similar trends for the base-flow component as for flood season flows and total flows, i.e. initial increase followed by reductions which are more significant under A2 compared to B2. The base-flow component reduces to less than 50% by the year 2090 for A2 compared to the mean of the base period. Although both flood season and baseflow are predicted to decrease by CGCM2, the reductions are relatively larger for the baseflow component allowing the proportion of flood season flows in the annual total to increase. ECHAM4 shows a general trend of increase under both scenarios but this time it is faster for the case of A2 than for the case of B2. Thus, the proportion of flood season flows in the annual total does not vary for A2 but increases slightly for B2.

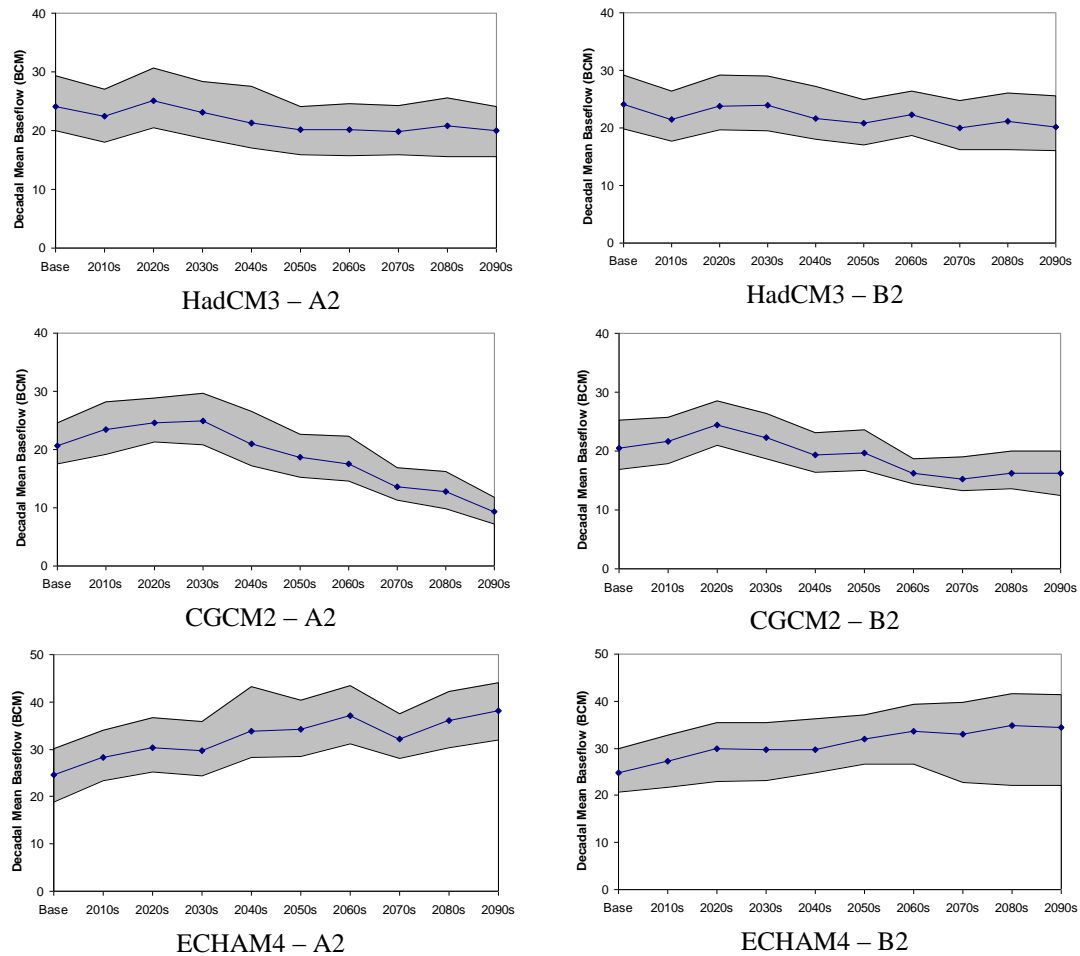


Figure 8: Simulated decadal mean base-flow at Dongola from 6 GCM experiments

6. CONCLUSIONS AND RECOMMENDATIONS

The following are the obtained conclusions from the present research:

- The absolute values of flows, generated from any of the GCM-based simulations, might be misleading because they do not originally reproduce the mean observed flow during the base period for both components and thus corrections might be necessary.
- The future trends were compared to the mean observed flow during the base period (1992-2001) and are given on Figure 9. From the figure, clear is that ECHAM4 predicts future increases in flows from both the Blue Nile/Atbara and the White Nile under both scenarios leading to increases in the total flow. But it should be noted that ECHAM4 highly underestimates the base-flow component for the base period. This indicates that the future trend might need correction.
- CGCM2 originally underestimates all flow components in the base-period and then predicts an increase for the two sub-basins by the decades 2020 and 2030 bringing the flows close to the observed mean then the flows decrease rapidly especially under the scenario A2.
- HadCM3 showed a slight upward trend for flood season flows and a slight downward trend for baseflow and thus the decadal mean total annual flow fluctuates around the base period flow. HadCM3 overestimates flood season flow in the base period and underestimates the baseflow component and thus the total is only slightly overestimated.
- The uncertainty range, Figure (9), across the models is larger than that across the two studied scenarios A2 and B2 for total flows, and for flows during the two designated seasons (flood season and baseflow). The range of differences between the scenarios is model dependent and time dependent. For example, CGCM2 predictions under both scenarios are close until the 2070s for total flow and for both seasons. The differences are minor for HadCM3 except for

flood season flow in the 2080s and 2090s, while differences are larger for ECHAM4 in the 2050s and 2060s then converge in the 2080s and 2090s.

- The uncertainty due to downscaling is also large and is proportional to the flow. It warrants increasing the ensemble size in order to use better statistical measures for the confidence interval than simply using the maximum and minimum.
- The implications of the changes might be huge for water resources planning and management within the basin and for Egypt. In case the future follows the expectations of ECHAM4, the predicted increases in flood season flow and base-flow could lead to larger floods which could be beneficial only if the right infrastructures were in place to store the excess water. For CGCM2, droughts are expected to occur more often, undermining development efforts. For HadCM3, changes are moderate for Egypt and could be handled but the increase in flood season flows will require some additional protection in Ethiopia and Sudan and the reduction in White Nile flows will require proper planning of conservation schemes in the sub-basins of the White Nile.

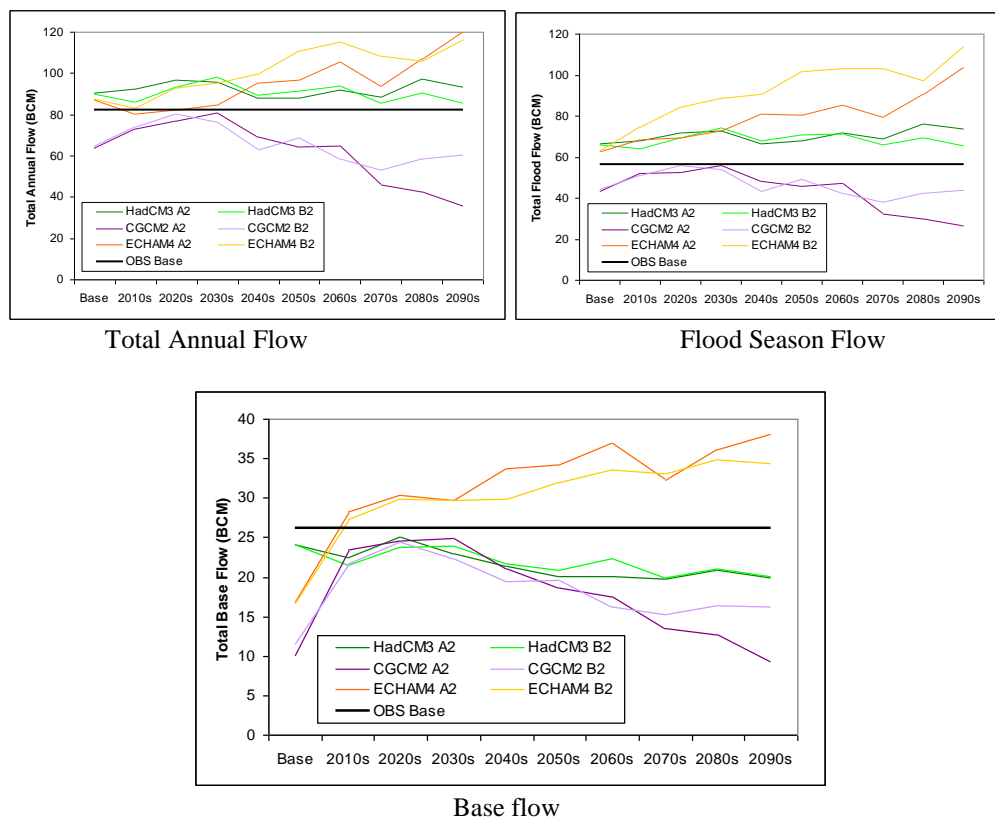


Figure9: Summary Intercomparison of Simulated decadal mean flows at Dongola from 6 GCM experiments

7. ACKNOWLEDGEMENTS

This study has been conducted as a sub-activity of the Dutch funded "Lake Nasser Flood and Drought Control" project. Technical assistance was provided to the project by a consortium led by WL|Delft Hydraulics. The Statistical Downscaling model was developed by Rizwan Nawaz (now at Leeds University UK) and Tim Bellerby from Hull University, UK, a part of the consortium. Several staff members of the NFC participated in the processing of input and output data and the running of the SDM.

8. REFERENCES

1. Abu-Zeid, M. and Biswas, A.K., 1991. *Some major implications of climatic fluctuations on water management*. International Journal of Water Resources Development, 7: 74-81.
2. Allen, R.G., Pereira, L.S., Raes, D. and Smith, M., 1998. *Crop evapotranspiration: Guidelines for computing crop water requirements*. FAO Irrigation and Drainage Paper No. 56. Food and Agriculture Organization of the United Nations, Rome.
3. Arnell, N.W., 1999. *Climate change and global water resources*. Global Environmental Change, 9(Supplement 1): S31-S49.
4. Bárdossy, A., 2000. *Stochastic Downscaling Methods to Assess the Hydrological Impacts of Climate Change on River Basin Hydrology*. In: J. Beersma, M. Agnew, D. Viner and M. Hulme (Editors), ECLAT-2. Climatic Research Unit, UEA, Norwich, UK, KNMI, The Netherlands, pp. 18-34.
5. Conway, D. and Hulme, M., 1993. *Recent fluctuations in precipitation and runoff over the Nile sub-basins and their impact on main Nile discharge*. Climatic Change, 25(2): 127-151.
6. Conway, D. and Hulme, M., 1996. *The Impacts of Climate Variability and Future Climate Change in the Nile Basin on Water Resources in Egypt*. International Journal of Water Resources Development, 13(3): 277-296.
7. Elshamy, M.E., Seierstad, I.A. and Sorteberg, A., 2008. *Impacts of climate change on Blue Nile flows using bias-corrected GCM scenarios*. Hydrol. Earth Syst. Sci. Discuss., 5(3): 1407-1439.
8. Elshamy, M.E.A.M., 2000. *Impacts of climate change on Nile flows*. Diploma of Imperial College (DIC) Thesis, Imperial College London, London.
9. Elshamy, M.E.A.M., 2006. *Improvement of the Hydrological Performance of Land Surface Parameterization: An Application to the Nile Basin*. PhD Thesis, Imperial College, University of London, London.
10. Eltahir, E.A.B., 1996. *El Niño and the Natural Variability in the Flow of the Nile River*. Water Resources Research, 32(1): 131-137.
11. Evans, T., 1990. *History of Nile Flows*. In: H.P. P. and A. J.A. (Editors), The Nile: Resource Evaluation, Resource Management, Hydropolitics and Legal Issues. SOAS-RGS, London, pp. 5-39.
12. Hulme, M., Doherty, R., Ngara, T., New, M. and Lister, D., 2001. *African climate change: 1900–2100*. Climate Research, 17: 145-168.
13. IPCC, 2000. *Special Report on Emission Scenarios*. Cambridge University Press, Cambridge, 570 pp.
14. Kite, G.W., 1981. *Recent Changes in Level of Lake Victoria*. Hydrological Sciences Bulletin, 26(3): 233-243.
15. LNFDC, 2008. *Nile Forecasting System (NFS)*, Project Final Report, Vol III, Planning Sector, Ministry of Water Resources and Irrigation, Giza, Egypt.
16. Mantoglou, A. and Wilson, J.L., 1982. *Turning bands method for simulation of random fields using line generation by a spectral method*. Water Resources Research, 18(5): 1379-1394.
17. Mohamed, Y.A., van den Hurk, B., Savenije, H.H.G. and Bastiaanssen, W.G.M., 2005. *Impact of the Sudd wetland on the Nile hydroclimatology*. Water Resources Research, 41(8): W08420.
18. Nile Forecast Center, 2007. *Nile Forecasting System software version 5.1*, Ministry of Water Resources and irrigation, Cairo, Egypt.
19. Raper, S.C.B. and Cubasch, U., 1996. *Emulation of the results from a coupled general circulation model using a simple climate model*. Geophysical Research Letters, 23(10): 1107-1110.
20. Said, R., 1993. *The River Nile: Geology, Hydrology, and Utilization*. Pergamon, Oxford, 320 pp.
21. Salathé, E.P., 2005. *Downscaling simulations of future global climate with application to hydrologic modelling*. International Journal of Climatology, 25(4): 419-436.
22. Sayed, M.A.-A., 2004. *Impacts of climate change on the Nile Flows*, Ain Shams University, Cairo, Egypt.
23. Sene, K.J., Tate, E.L. and Farquharson, F.A.K., 2001. *Sensitivity studies of the impacts of climate change on White Nile flows*. Climatic Change, 50(1-2): 177-208.
24. Shahin, M., 1985. *Hydrology of the Nile Basin*. Developments in water science ; 21. Elsevier, Amsterdam ; Oxford.
25. Soliman, E.S.A., Sayed, M.A.-A., Nour El-Din, M. and Samy, G., 2008. *Integration of NFS with Regional Climate Model to Simulate the Nile Basin Hydro-climatology*. Nile Basin Water

- Engineering Scientific Magazine, 1: 75-85.
26. Strzepek, K.M., Onyeji, S.C., Saleh, M. and Yates, D., 1995. *An Assessment of Integrated Climate Change Impacts on Egypt*. In: K.M. Strzepek and J. Smith (Editors), *As Climate Changes: International Impacts and Implications*. Cambridge University Press, Cambridge, UK, pp. 180-200.
 27. Sutcliffe, J.V. and Lazenby, J.B.C., 1990. *Hydrological data requirements for planning Nile management*. In: P.P. Howell and J.A. Allan (Editors), *The Nile, Resource Evaluation, Resource Management, Hydropolitics and Legal Issues*. SOAS/RGS, London, pp. 107-136.
 28. Sutcliffe, J.V. and Parks, Y.P., 1999. *The hydrology of the Nile*. IAHS Special Publication No. 5. International Association of Hydrological Sciences, Wallingford, UK.
 29. Widmann, M., Bretherton, C.S. and Salathé, E.P., 2003. *Statistical Precipitation Downscaling over the Northwestern United States Using Numerically Simulated Precipitation as a Predictor*. *Journal of Climate*, 16(5): 799-816.
 30. Yates, D., 1996. *Integrating Water into an Economic Assessment of Climate Change Impacts on Egypt*. Working Paper WP-96-31, IIASA, Austria.